

**TIME DOMAIN QUANTIFICATION OF AMPLITUDE, CHEMICAL SHIFT,  
APPARENT RELAXATION TIME  $T_2^*$  AND PHASE BY WAVELET  
TRANSFORM ANALYSIS: APPLICATION TO BIOMEDICAL MAGNETIC  
RESONANCE SPECTROSCOPY**

HACENE SERRAI\*, LOTFI SENHADJI#, JACQUES D. DE CERTAINES\* AND  
JEAN. LOUIS. COATRIEUX#.

*\* Laboratoire de Résonance Magnétique en Biologie et Médecine, Faculté de  
Médecine, F-35043 RENNES Cedex, France.*

*# L.T.S.I, INSERM, Campus Scientifique de Beaulieu, F-35042 RENNES Cedex,  
France.*

## ABSTRACT

Wavelet Transform (WT) was used to quantify the Magnetic Resonance Spectroscopy (MRS) parameters, chemical shift, apparent relaxation time  $T_2^*$ , resonance amplitude and phase. Wavelet Transform is a time-frequency representation which separates each component from the FID, which is then successively quantified and subtracted from the raw signal. Two iterative procedures were developed. They were combined with a nonlinear regression analysis method and tested on both simulated and real sets of biomedical MRS data selected with respect to the main problems usually encountered in quantifying biomedical MRS, specifically "chemical noise" resulting from overlapping resonances and baseline distortion. The results indicate that the Wavelet Transform method can provide efficient and accurate quantification of MRS data.

## INTRODUCTION

Wavelet Transform (WT), as proposed by Grossmann and Morlet (*1*), analyzes a non-stationary signal by transforming its input time domain into a time-frequency domain. Through translation and dilation operations, WT decomposes the signal according to a set of functions, all deduced from a unique prototype called wavelet, assumed to be well localized both in time and frequency domains. Such a time-frequency representation could provide a more efficient solution than usual Fourier Transform (FT) or other new methods presently available to process MRS data (2-5).

WT is presented here as a quantification method in biomedical MRS with special attention to the FID signal characteristics. FID signal considered as a sum of damped sinusoids is analyzed by WT and decomposed to its different components. The components are then successively separated with respect to their time durations and resonance frequencies, quantified and subtracted from the raw signal. Chemical shift and phase values, are estimated from the WT phase information, while the WT modulus is used to estimate the values of amplitude resonance  $A$  and apparent relaxation time  $T_2^*$ . The problems often encountered in biomedical MRS applications, low signal-to-noise ratio, broad resonances, and "chemical noise", can then be reduced and accurate estimation of MRS parameter values may be obtained.

Two iterative procedures obtained from the application of WT on noise-free MRS signals composed of one and two resonances respectively are tested on simulated and real biomedical MRS data. The case of noisy signals is considered and a classical solution is proposed.

## CONTINUOUS WAVELET TRANSFORM

Let  $L^2(\mathbb{R})$  be the vectorial space of the square integrable functions, i.e signals of finite energy. For  $u(t)$  and  $v(t)$  belonging to  $L^2(\mathbb{R})$ , the scalar product between  $u$  and  $v$  is given by :

$$\langle u, v \rangle = \int u(t)v^*(t)dt \quad [1]$$

Asterisk denotes the complex conjugate.

For any function  $u(t)$  of  $L^2(\mathbb{R})$ ,  $\hat{u}(\omega)$  is the associated Fourier Transform defined by :

$$\hat{u}(\omega) = \int_{-\infty}^{+\infty} u(t)e^{-i\omega t} dt \quad [2]$$

Any function  $g(t)$  belonging to  $L^2(\mathbb{R})$  is called an analyzing wavelet if it complies with the so-called admissibility condition ( $\mathcal{O}$ ):

$$C_g = \int_{-\infty}^{+\infty} \frac{|\hat{g}(\omega)|^2}{|\omega|} d\omega < \infty \quad [3]$$

With respect to this wavelet, the continuous wavelet transform of a signal  $s(t)$  of finite energy is given by :

$$S_a(b) = \langle s, g_{a,b} \rangle = \frac{1}{a} \int s(t)g^*\left(\frac{t-b}{a}\right)dt \quad [4]$$

with  $g_{a,b}(t) = \frac{1}{a}g\left(\frac{t-b}{a}\right)$ ,  $a > 0$ ,  $b \in \mathbb{R}$ .

It maps the signal via a two-dimensional function on the time-scale domain plane (a, b). This operation is equivalent to a particular filter bank analysis, whose relative frequency band widths are constant and related to the parameters a and b (scale parameter and translation parameter) and to the frequential properties of the wavelet g.  $S_a(b)$  can indeed be written as :

$$S_a(b) = \int s(t) \tilde{g}_a(b-t) dt \quad [5]$$

where  $\tilde{g}_a(\cdot) = \frac{1}{a} g^*\left(-\frac{\cdot}{a}\right)$  is the impulse response of the filter.

There is a large set of functions satisfying the required condition of Eq. [3] : not only can the analyzing wavelet be selected to the signal features but the parameters a and b can be adjusted without, limiting their range values. Transient events, lying in a specific frequency domain, can then be easily targeted. In practice, to achieve satisfactory signal analysis, regularity and a suitable time-frequency band width product are required for g. So far, the most commonly used analyzing wavelet is the so-called Morlet wavelet defined by :

$$g(t) = e^{-\frac{t^2}{2}} e^{i\omega_0 t} + c(t) \quad [6]$$

where c(t) is a correcting term ensuring the admissibility condition. For  $\omega_0 > 5$ , the term c(t) is negligible and g(t) is practically admissible, where  $\hat{g}(\omega) \approx 0$  if  $\omega \leq 0$  (7).

In the next section, the concept of wavelet transform, briefly recalled here, is considered in MRS signal analysis and quantification.

## DEVELOPMENT OF A METHOD FOR MRS SIGNAL PROCESSING

Quantification is a necessary step for clinical implementation of large-scale MRS. However, due to specific problems related to biomedical data such as broad spectral lines, overlapping resonances and poor signal-to-noise ratio (SNR), absolute quantification remains a difficult challenge for currently available data processing methods. Wavelet Transform, would appear to be an alternative method to the traditional FT for MRS data quantification. The elementary components of the FID signal are successively separated, quantified and subtracted from the raw signal.

Referring to (8), the FID signal, considered here as a noise-free signal, is composed of a sum of damped complex sinusoids decaying with time and may be written as :

$$s(t) = \sum_{j=1}^N A_j e^{\left(\frac{-t}{T_{2j}^*}\right)} e^{i(\omega_j t + \varphi_j)} = \sum_{j=1}^N s_j(t) \quad [7]$$

where  $A_j$ ,  $T_{2j}^*$ ,  $\omega_j = 2\pi\delta_j$  and  $\varphi_j$  are the resonance amplitude, apparent relaxation time, angular frequency (chemical shift  $\delta_j$ ) and phase, respectively, of the component  $s_j$ .  $N$  denotes the total number of the signal resonances. We assume here, as is generally the case, that the damping factor of each component given by  $\frac{1}{\pi T_{2j}^*}$  is very small compared with  $\omega_j$ .

*Case of signal with one component*

According to [7], the FID signal may be written as :

$$s(t) = Ae^{(-t/T_2^*)} e^{i(\omega_s t + \varphi)} \quad [8]$$

Our aim is to estimate the values of the MRS parameters. Due to the causality of the FID signal, our conventions for the time-frequency domain display are the same as in (9),  $(a, b \in \mathbb{R}^+ \times \mathbb{R}^+)$ , (Fig. 1).

According to Eq. [4], the WT of  $s(t)$  with respect to the Morlet wavelet is given by :

$$S_a(b) = \frac{1}{a} \int_0^{+\infty} Ae^{\left(\frac{-t}{T_2^*}\right)} e^{i(\omega_s t + \varphi)} e^{\left(\frac{-(t-b)^2}{2}\right)} e^{-i\omega_0 \left(\frac{t-b}{a}\right)} dt \quad [9]$$

Substituting  $u$  for  $(t-b)/a$ ,  $S_a(b)$  becomes :

$$S_a(b) = Ae^{\left(\frac{-b}{T_2^*}\right)} e^{i(\omega_s b + \varphi)} \int_{-b/a}^{\infty} e^{\left(\frac{-au}{T_2^*}\right)} e^{i(a\omega_s - \omega_0)u} e^{\left(\frac{-u^2}{2}\right)} du = s(b).J \quad [10]$$

Taking  $\Delta$  as :

$$\Delta = a\omega_s - \omega_0 \quad [11]$$

one can check that the quantity  $J$  given by  $\int_{-b/a}^{\infty} e^{\left(\frac{-au}{T_2^*}\right)} e^{i\Delta u} e^{\left(\frac{-u^2}{2}\right)} du$  is equivalent to :

$$J = e^{\frac{1}{2}\left(\frac{a}{T_2^*}\right)^2} e^{(-i\Delta \frac{a}{T_2^*})} \int_{\alpha}^{\infty} e^{\left(\frac{-t^2}{2} + i\Delta t\right)} dt = e^{\frac{1}{2}\left(\frac{a}{T_2^*}\right)^2} e^{(-i\Delta \frac{a}{T_2^*})} .I \quad [12]$$

$$\alpha = \left( \frac{a}{T_2^*} - \frac{b}{a} \right)$$

with

If I is given its value in Appendix 1, the expression of  $S_a(b)$  becomes :

$$S_a(b) = s(b) e^{\frac{1}{2} \left( \frac{a}{T_2^*} \right)^2} e^{-i \Delta \frac{a}{T_2^*}} [B + iC] \quad [13]$$

The terms B and C are the result of board effects of the projection of the signal onto the quart plane H along the axis where  $b = 0$ .

If we represent the result of the WT of Eq. [13] in terms of modulus and phase, we obtain :

$$S_a(b) = |S_a(b)| e^{i\Phi_a(b)} \quad [14]$$

The modulus contains A and  $T_2^*$ , it is given by :

$$|S_a(b)| = A e^{\left( \frac{a^2}{2T_2^{*2}} - \frac{b}{T_2^*} \right)} \sqrt{B^2 + C^2} . \quad [15]$$

The phase of  $S_a(b)$ , containing  $\omega$  and  $\varphi$  of the signal is given by :

$$\Phi_a(b) = \omega_s b + \varphi - \Delta \frac{a}{T_2^*} + \text{Arctg} \frac{C}{B} \quad [16]$$

Because of the terms B and C in the modulus and the phase, it is difficult to compute the values of MRS parameters.

Note that if  $\Delta = 0$ , the term C is null (see Appendix 1), the phase  $\Phi_a(b)$  in Eq. [16] becomes equal to the phase of the signal. This condition is fulfilled if  $\omega_s$  is known. Unfortunately this is not the case. One can estimate the value of  $\omega_s$  and approach  $\Delta = 0$  by the following procedure.

Let us take the two first terms of the series  $U_k$  in Appendix 1. The term B is restricted to :

$$B = \sqrt{\frac{\pi}{2}} e^{\frac{-\Delta^2}{2}} m \sqrt{\frac{\pi}{2}} \sqrt{1 - e^{-\alpha^2}} \quad [17]$$

and C becomes :

$$C = \pm \sqrt{\frac{\pi}{2}} e^{\frac{-\Delta^2}{2}} (\sqrt{e^{\Delta^2} - 1}) - \Delta (1 - e^{\frac{-\alpha^2}{2}}) \quad [18]$$

The signs  $m$  in Eq. [17] and  $\pm$  in Eq. [18] are conditioned by the signs of  $\alpha$  and  $\Delta$  respectively.

Consider now  $\Omega_a(b) = \frac{d\Phi_a(b)}{db}$  as the instantaneous frequency of  $S_a(b)$ . Combining

Eqs. [16], [17] and [18],  $\Omega_a(b)$  may be written as :

$$\Omega_a(b) = \frac{d\Phi_a(b)}{db} = \omega_s + \frac{d(\text{Arctg}(\frac{C}{B}))}{db} \quad [19]$$

For a given value of the dilation parameter  $a$  of the wavelet, noted  $a_0$ , a value of the

translation parameter  $b$  exists, noted  $b_r$ , such that for any  $b > b_r$ , the term  $\frac{d(\text{Arctg}(\frac{C}{B}))}{db}$

in Eq. [19] is negligible (see Appendix 2). A first estimation of  $\omega_s$  is then obtained from :

$$\Omega_{a_0}(b_0) \approx \omega_s \quad b_0 > b_r \quad [20]$$

The value of the translation parameter  $b_0$  indicates that  $\omega_s$  is estimated at the end of the FID signal (at the last points of the corresponding sampled signal).

To have more precision on the estimated value of  $\omega_s$ ,  $\Delta$  should be closer to zero. In practice, this is obtained iteratively by the following, (Fig. 2).

Substitute  $\Omega_{a_0}(b_0)$  for  $\omega_s$  in Eq. [11] and assume  $\Delta$  equals zero. The new value  $a_1$  of the dilation parameter is computed by :

$$a_1 = \frac{\omega_0}{\Omega_{a_0}(b_0)} \quad [21]$$

The new calculated value of the instantaneous frequency  $\Omega_{a_1}(b_0)$  associated to  $S_{a_1}(b_0)$  is closer to  $\omega_s$ . The iterative procedure converges within some iterations when the following condition is fulfilled :

$$\left| \frac{a_{j+1} - a_j}{a_j} \right| < \varepsilon \quad [22]$$

where  $a_j$  is the value of the dilation parameter obtained at the iteration  $j$ .  $\varepsilon$  is an arbitrarily small fixed positive number.

Once this first iterative procedure converges, the value of  $\omega_s$  is estimated from  $\Omega_{a_r}(b_0)$ , where  $a_r$  is the final value of the dilation parameter  $a$  at convergence.  $\Delta$  approaches zero and this automatically implies that  $C$  decreases to zero and that  $B$  is

restricted to  $\sqrt{\frac{\pi}{2}} \left[ 1 m \sqrt{1 - e^{-\alpha^2}} \right]$ . Consequently,  $S_{a_r}(b)$  becomes :

$$S_{a_r}(b) = \sqrt{\frac{\pi}{2}} e^{\frac{1}{2} \left( \frac{a_r}{T_2} \right)^2} \left[ 1 m \sqrt{1 - e^{-\alpha^2}} \right] A e^{\left( \frac{-b}{T_2} \right)} e^{i(\omega_s b + \varphi)} \quad [23]$$

The phase  $\varphi$  of the FID signal is directly estimated from the phase of  $S_{a_r}(b)$  and a simple nonlinear regression algorithm (14-16) applied on the modulus gives the estimated values of  $A$  and  $T_2^*$ .

$S_{a_r}(b)$  is now equal to the signal at every point  $t = b$  up to a known function  $F(b)$  given by :

$$F(b) = \sqrt{\frac{\pi}{2}} e^{\frac{1}{2} \left( \frac{a_r}{T_2^*} \right)^2} \left[ 1 m \sqrt{1 - e^{-\alpha^2}} \right] \quad [24]$$

This development allows us to generalize the procedure to a noise-free signal composed of more than one component.

#### *Case of signal composed of more than one component*

Now let  $s(t)$  be a FID signal composed of two resonances given by :

$$s(t) = A_1 e^{\frac{-t}{T_{21}}} e^{i(\omega_1 t + \varphi_1)} + A_2 e^{\frac{-t}{T_{22}}} e^{i(\omega_2 t + \varphi_2)} = s_1(t) + s_2(t) \quad [25]$$

WT of  $s(t)$  with respect to the Morlet wavelet, is :

$$S_a(b) = \frac{1}{a} \int_0^{\infty} e^{\frac{-(\frac{t-b}{a})^2}{2}} e^{-i\omega_0 \frac{t-b}{a}} \left[ A_1 e^{\frac{-t}{T_{21}}} e^{i(\omega_1 t + \varphi_1)} + A_2 e^{\frac{-t}{T_{22}}} e^{i(\omega_2 t + \varphi_2)} \right] dt \quad [26]$$

Following the same development as in the previous subsection, we obtain :

$$S_a(b) = |S1_a(b)| e^{i\Phi1_a(b)} + |S2_a(b)| e^{i\Phi2_a(b)} \quad [27]$$

This representation of  $s(t)$  is considered as a sum of two wavelet transforms each one associated to one particular component of the signal and described as in Eq. [14] by its modulus and phase.

WT has to be adapted to this type of signal in order to isolate the components from the FID and to estimate their MRS parameter values.

If we write Eq. [27] according to the WT associated to the first component  $S_1$ , we obtain :

$$S_a(b) = |S1_a(b)| e^{i\Phi1_a(b)} \left[ 1 + Z_a(b) e^{i\Theta_a(b)} \right] \quad [28]$$

The interference terms resulting from the interactions between the two components are represented by  $Z_a(b)$ , where :

$$Z_a(b) = \frac{|S2_a(b)|}{|S1_a(b)|} \quad [29]$$

and  $\Theta_a(b)$  which is equal to :

$$\Theta_a(b) = \Phi2_a(b) - \Phi1_a(b). \quad [30]$$

If we substitute Eqs. [15] and [16] for the moduli and phases in Eqs. [29] and [30] respectively, we notice that the degree of interactions between the components depends particularly on the ratio  $\frac{A_2}{A_1}$  and the difference  $\omega_2 - \omega_1$ .

Suppose now that the first component  $s_1$  decays more slowly than the second one ( $T_{2_1}^* > T_{2_2}^*$ ), (Fig. 3). For a given translation parameter value  $b$  of the wavelet, noted also  $b_r$ , the remaining component in the signal for any  $b > b_r$  is the first one. WT of  $s(t)$  is reduced to :

$$S_a(b) = |S1_a(b)|e^{i\Phi1_a(b)} \quad b > b_r \quad [31]$$

By comparing Eq. [31] and Eq. [28], the quantity  $Z_a(b)e^{i\Theta_a(b)}$  describing the component interactions becomes negligible for  $b > b_r$ . This allows us to use the first iterative procedure, to estimate the value of  $\omega_1$  and to compute  $a_r$ , i.e the final value of the dilation parameter fulfilling Eq. [22]. At the convergence of the iterative procedure, the frequency of the component having the greatest apparent relaxation time  $T_2^*$  value is localized at the wavelet parameter values  $b > b_r$  and  $a = a_r$ . As a result, the corresponding WT according to Eq. [23] is given by :

$$S_{a_r}(b) = \sqrt{\frac{\pi}{2}} e^{\frac{1}{2} \left(\frac{a_r}{T_{2_1}^*}\right)^2} \left[ 1 \ m \sqrt{1 - e^{-\alpha_1^2}} \right] A_1 e^{\left(\frac{-b}{T_{2_1}^*}\right)} e^{i(\omega_1 b + \varphi_1)} \quad b > b_r \quad [32]$$

The sign  $m$  is conditioned by the sign of  $\alpha_1$  given by  $\alpha_1 = \left(\frac{a_r}{T_{2_1}^*} - \frac{b}{a_r}\right)$ .

Choosing a very large value of the translation parameter  $b$ , for example  $b_0$  ( $b_0 > b_r$ ) allows computation of  $\varphi_1$  value from the phase of Eq. [32]. To estimate the values of  $A_1$  and  $T_{2_1}^*$ , the modulus is stored on  $M$  points and fitted to its expression in Eq. [32] by a nonlinear regression algorithm. Unfortunately, it is difficult to determine the number  $M$ .  $M$  decreases when the value of  $b_r$  which is connected to the unknown value of  $T_{2_2}^*$  increases. Furthermore, to have an accurate estimation, the number  $M$  should be as large as possible, which is not generally the case if  $T_{2_2}^*$  is close to  $T_{2_1}^*$ , even if the value of  $T_{2_2}^*$  is known. To solve this problem, the first component has to be separated from the signal. The interactions between the components are to be investigated from their frequency difference or their amplitude ratio. Here we observe the frequency difference as it is easier to obtain. Two situations have to be considered.

1) If the frequencies of the two components are sufficiently far away from each other, the fast decay of  $\hat{g}$  will allow us to treat the first component independently from the second one. The interactions between the components are practically non-existent, their corresponding  $Z_a(b) e^{i\Theta_a(b)}$  quantity in Eq. [28] is null.  $S_{a_r}(b)$  of Eq. [32] becomes valid to every point  $b$ , allowing an estimation of the values of  $A_1$  and  $T_{2_1}^*$  from its

modulus and separation of the first component from the signal in order to subtract it out.

2) If the difference between the two frequencies is small, case of overlapping resonances, the quantity  $Z_a(b)e^{i\Theta_a(b)}$  is not null. It prevents us from treating the first component independently from the second one. The values of  $A_1$  and  $T_{2_1}^*$  are estimated with respect to the contribution of the second component. The full WT  $S_a(b)$  of Eq. [28] should be computed for  $a = a_r$ . With respect to the  $a_r$  value involving  $\Delta_1 = 0$  and  $C1 = 0$  for the phase  $\Phi_{1_{a_r}}(b)$  in Eq. [30],  $\Theta_{a_r}(b)$  becomes :

$$\Theta_{a_r}(b) = (\omega_2 - \omega_1)b + (\varphi_2 - \varphi_1) - \frac{a_r \Delta_2}{T2_2^*} + \text{Arctg}\left(\frac{C2_{a_r}(b)}{B2_{a_r}(b)}\right) \quad [33]$$

The dominant term in Eq. [33] is  $(\omega_2 - \omega_1)b$ . Referring to (17), and due to the small difference between  $\omega_1$  and  $\omega_2$ , the values of the other terms may be neglected.  $\Theta_{a_r}(b)$  is approximated by :

$$\Theta_{a_r}(b) \approx (\omega_2 - \omega_1)b \quad [34]$$

Substituting  $\Theta_{a_r}(b)$  in Eq. [28],  $S_{a_r}(b)$  is approximated by :

$$S_{a_r}(b) \approx |S_{1_{a_r}}(b)| \sqrt{1 + Z_{a_r}^2(b) + 2Z_{a_r}(b)\cos((\omega_1 - \omega_2)b)} \cdot e^{i(\Phi_{1_{a_r}}(b) + \Psi_{a_r}(b))} \quad [35]$$

With  $\Psi_{a_r}(b) = \text{Arctg}\left(\frac{R_{a_r}(b)}{T_{a_r}(b)}\right)$  where  $R_{a_r}(b) = Z_{a_r}(b)\sin((\omega_2 - \omega_1)b)$  and  $T_{a_r}(b) = 1 + Z_{a_r}(b)\cos((\omega_2 - \omega_1)b)$ .

The applied nonlinear regression algorithm on the modulus of Eq. [35] allows us to estimate not only the values of  $A_1$  and  $T_{21}^*$ , but also the parameter values of  $A_2$ ,  $T_{22}^*$  and  $\omega_2$  of the contributing second component  $s_2$  in  $S_{a_r}(b)$ .

The estimated value of  $A_2$  represents here the amount of the contribution of the second component in  $S_{a_r}(b)$ , and not the total amplitude resonance of  $s_2$  in the signal  $s(t)$ . If  $\omega_2$  is far from  $\omega_1$ ,  $s_2$  contributes little in  $S_{a_r}(b)$  and its  $A_2$  estimated value is small compared with the total amplitude resonance of  $s_2$ . Inversely, if  $\omega_2$  is close to  $\omega_1$  the estimated value of  $A_2$  becomes larger.

To separate the first component  $s_1$  from the signal, the terms  $Z_{a_r}(b)$  and  $\Psi_{a_r}(b)$  should be negligible in Eq. [35]. Note that the value of  $Z_{a_r}(b)$ , according to Eq. [29] is negligible if the value of  $A_2$  is small compared with the value of  $A_1$ .

By enforcing the resolution of the wavelet in the frequency domain, the wavelet  $\hat{g}$  decays faster. Its frequency band is narrowed and focused around the frequency of the first component.  $S_{a_r}(b)$  is smoothed, containing mainly the first component. The influence of the second component is reduced. The component  $s_1$  may be separated and filtered from the signal  $s(t)$ . The more the frequency resolution of the wavelet is enhanced, the more the contribution of the second component is attenuated. The enhancement of the frequency resolution of the wavelet is limited by the signal duration. The support of the wavelet in the time domain becomes wider.

It can be practically proceeded as follows, (Fig. 4). Multiply the values of  $a_r$  and  $\omega_0$  by a given positive factor  $f$  ( $f > 1$ ) to enhance the frequency resolution of the wavelet and

keep its central frequency constant ( $\Delta_1 = 0 \Rightarrow \omega_1 = \frac{f \cdot \omega_0}{f \cdot a_r}$ ). Compute the smoothed  $S_{f.a_r}(b)$ . The values of  $A_1$ ,  $T_{2_1}^*$ ,  $A_2$ ,  $T_{2_2}^*$  and  $\omega_2$  are estimated from the modulus of Eq.

[35].  $A_1$  is compared with  $A_2$ . If the condition  $\left| \frac{A_2}{A_1} \right| < \varepsilon$  is fulfilled, the procedure stops. Otherwise, the factor  $f$  is increased and a new iteration begins by executing the same steps as above. At the convergence of this second procedure, the final estimated value of  $A_2$  is small compared with the value of  $A_1$ . The terms  $Z_{f.a_r}(b)$  and  $\Psi_{f.a_r}(b)$  become negligible in Eq. [35] and  $S_{f.a_r}(b)$  may be approximated to :

$$S_{f.a_r}(b) \approx \sqrt{\frac{\pi}{2}} A_1 e^{\left( \frac{a_r^2}{2(T_{2_1}^*)^2} - \frac{b}{T_{2_1}^*} \right)} \left[ 1 - m(1 - e^{-\alpha_1^2})^{\frac{1}{2}} \right] e^{i(\omega_1 b + \phi_1)} \quad [36]$$

The WT described by Eq. [36] is equal to the first component  $S_1$  of the signal at every point  $t = b$  up to a known function  $F_1(b)$  similar to Eq. [24]. The separated component is subtracted from the signal with respect to  $F_1(b)$  and the second component of the signal is quantified using only the first procedure.

This development may be extended on a FID signal containing more than two components. The proposed solutions are included in a third iterative procedure. The number of iterations of this third procedure will be equal to the number of signal components. At each iteration, the frequency of the largest time component among the remaining components in the signal is detected. The effects of the component

interactions are reduced. The isolated component is quantified and extracted from the raw signal.

### *Case of noisy signal*

The random noise encountered in the FID signal largely originates from thermal noise in the probe and early stages of the receiver during data acquisition. FID decays with time, while the noise amplitude remains constant. In some cases the amplitude of noise is important and may complicate detection of the resonances.

An efficient method for increasing the SNR consists in multiplying the data by a decreasing exponential function, written as follows :

$$f(t) = e^{\left(\frac{-t}{T}\right)} \quad [37]$$

Where  $T > 0$  is the constant time of the window function  $f(t)$ . The desired reduction in the size of the tail of the signal occurs. Sensitivity is enhanced by using this filter. Multiplication in this fashion speeds up the apparent decay of the signal, given by :

$$\frac{1}{T_2^a} = \frac{1}{T_2^*} + \frac{1}{T} \quad [38]$$

The estimation of the frequency components at the end of the signal is still possible by using the first iterative procedure, (see Fig. 5 adapted from (18)) and according to the frequency difference between the components, the second iterative procedure is used to estimate  $A$  and  $T_2^*$  values.

To recover the values of the apparent relaxation time, the following relation is used :

$$\frac{1}{T_2^*} = \frac{1}{T_2^a} - \frac{1}{T} \quad [39]$$

## APPLICATION TO SIMULATED MRS DATA

To test the accuracy and the efficiency of the proposed quantification technique, FIDs were simulated by a home PC software according to Eq. [7] and quantified by WT. The sampling frequency was normalized to 1. Each simulated signal was stored on 1024 points. To have an accurate estimation of A and  $T_2^*$  values, the order of the series  $U_k$  of the terms B2 and C2 contained in  $|S_{2_{a_r}}(b)|$ , was chosen to be equal to 10. The start value of the analyzing frequency  $\omega_0$  of the wavelet was chosen as greater than 5, set to 11. The initial values of the dilation parameter  $a_0$  and the factor f were taken to equal 1 and 2 respectively. The precision order of the two iterative procedures was supported by the value of  $\varepsilon$  set to 0.001. The estimated and reference MRS parameter values, the chosen value of  $b_0$ , the obtained value of  $a_r$  after convergence of the iterative procedures, and the requested number of iterations, noted j, for each signal component are reported on tables 1, 2 and 3.

*Case of a signal with one component* : The aim of this first simple test was to investigate the behavior of the WT quantification method and to check the number of requested iterations. Six simulated signals, each containing one component, were quantified (Fig. 6A). For each signal, the translation parameter point  $b_0$  was chosen and the first iterative procedure applied. It converged and stopped at the final value  $a_r$ , fulfilling Eq. [22]. The frequency of the signal and its phase were estimated. The

nonlinear analysis algorithm was used to fit the modulus to its expression and to give the values of  $A$  and  $T_2^*$  (Fig. 6B). The results obtained are reported on Table 1.

*Case of two overlapping resonances* : This case is often encountered in biomedical MRS, for instance in the in-vitro high resolution 1H MRS of body fluids or in in-vivo 31P MRS of brain tissue. Three simulated signals (A, B and C) were quantified, each one composed of two overlapping resonances. The results obtained are reported on Table 2.

For the first signal (Fig. 7A), the first iterative procedure was applied. The translation parameter point  $b_0$  was chosen to equal 300. We assumed that for  $b \geq 300$ , the remaining resonance in the signal is the longest one (say the first one). At the convergence of the procedure, the linear parameter values  $\omega_1(\delta_1)$  and  $\varphi_1$  of the first component were estimated. The second iterative procedure was used to estimate the parameter values of  $A_1$  and  $T_{2_1}^*$  of the localized first component and to separate it from the signal. It stopped when the estimated value of  $A_2$  reaches 0.08 which satisfies the

condition  $\left| \frac{A_2}{A_1} \right| < \varepsilon$ . The number of iterations of this second procedure depends on the degree of the component interactions. For this example, the procedure stopped at the twentieth frequency wavelet enhancement ( $f=20$ ). Note that at each iteration, the estimated values of  $A_1$ ,  $T_{2_1}^*$  and  $T_{2_2}^*$  varied little, whereas the estimated value of  $A_2$  decreased. This demonstrates that the contribution of the second component was reduced when the frequency resolution of the wavelet was enhanced. The change noted in the shape of the modulus of the first component shown in Fig. 7B, after the application of the second procedure, is another confirmation of this assumption. The

first separated component was filtered from the signal and the parameter values of the second component were estimated using only the first iterative procedure.

In signal B (Fig. 7C), the aim was to extract the narrow peak from a broad baseline containing a large peak (a short  $T_2^*$  value). The same steps as used previously were repeated. The translation parameter point  $b_0$  was chosen equal to 150. The longest component (in time) was first quantified and subtracted from the raw signal by applying the first and second procedure respectively. The second procedure, due to the small difference in frequency between the components and the large value of the amplitude resonance  $A_2$ , took more time to converge ( $f=6$ ). After subtraction of the first component from the signal, the second one was quantified by applying only the first iterative procedure (Fig. 7C).

In the last example (Fig. 7D), the resonances were large and had amplitudes and  $T_2^*$  values close to each other. This test is presented to illustrate the capacity of the WT method to separate two large resonances as in the  $^1\text{H}$  MRS signal of alkyl region of the plasma lipoprotein. For this example, the frequency difference between the two components was large enough so that the first iterative procedure alone gave satisfactory quantification of the two resonances.

*Case of noisy signal :* The low-pass filter was introduced in this test to obtain a satisfactory SNR in order that the quantification procedures would remain valid.

A noise-free signal, containing two components and three similar signals with additive complex noise, with noise variance  $\sigma_n$  equal to 200, 300 and 400 respectively, were simulated, (Fig. 8A). The injected noise in the signals is white and uniform. The low-pass filter was first applied on each signal to enhance the SNR with filter time constant

T equal to 145 ms, 80 ms and 50 ms respectively (Fig. 8B). Due to the large difference between the frequencies of the two components in signals 1 and 2, only the first iterative procedure was used to quantify the components. For signals 3 and 4, the components became large and overlapped in the frequency domain. To separate them, the second iterative procedure was needed. The MRS parameter values of the two components were estimated for each signal and given in Table 3.

The correlation coefficients between reference values of  $\delta$ , A and  $T_2^*$ , and the corresponding WT estimations were calculated on the 20 simulated resonances : 6 sets of data with one resonances (Table 1, Fig. 6), 3 sets of data with two overlapping resonances (Table 2, Fig. 7) and 4 sets of data with two resonances and varying noise levels (Table 3, Fig. 8). The correlation coefficients are 0.985, 0.999 and 0.989 for A,  $\delta$ , and  $T_2^*$  respectively. The noise level appeared to be the most disturbing factor, with more effect on A and  $T_2^*$  than on  $\delta$  (Fig. 9).

#### APPLICATION TO REAL BIOMEDICAL MRS DATA

In order to further demonstrate the usefulness of the WT method in biomedical MRS, a selected example is presented to illustrate the potential of WT. In this example, a set of FIDs resulting from a  $^{31}\text{P}$  MRS experiment on perfused working smooth muscle was considered. The set contains six peaks: PME, Pi, PCr a common reference peak at 0 ppm,  $\gamma$ ,  $\alpha$  and  $\beta$ -ATP. The  $^{31}\text{P}$  MRS was performed at 202.45 MHz on Avance DMX500 Spectrometer (Bruker, Wissenbourg, France). FIDs were acquired with 14.5  $\mu$  sec pulse, 1200 accumulations, a  $\pm$  5000 Hz spectral width and 32K data

points. A 20 Hz line broadening was applied before processing data to enhance the SNR. Fig. 10 shows the corresponding spectrum.

The results obtained by WT (Table 4) were compared to those obtained by a Bruker Spectral Fitting Method (UXNMR 1D, Bruker) and a time-domain method called Variable Projection Method (VARPRO) (21-22). Only the first 1024 FID points were processed by both WT and VARPRO, whereas the Spectral Fitting method fit all the data points to a lorentzian model. Unlike the other two methods, WT did not require baseline or phase corrections before quantification nor any prior knowledge.

## CONCLUSION

A quantification method based on Wavelet Transform analysis has been proposed. Described by two iterative procedures and a nonlinear regression analysis algorithm, the technique presented is the combination of linear and nonlinear methods. As an alternative method to the Fourier Transform, Wavelet Transform appears efficient in obtaining accurate estimation of the values of the MRS parameters  $\delta$ ,  $T_2^*$ , A and  $\varphi$  of each signal component.

We clarified the determining role of the apparent relaxation time  $T_2^*$  in estimating the chemical shift. The first iterative procedure supported by the information obtained from the phase of the wavelet signal representation, achieved this operation successfully. Extraction of the components from the signal depended on component interactions. We have shown that the amplitude ratio and the frequency difference between the components determine their degree of interaction. The second iterative procedure proposed manipulates the frequency content of the WT by using the wavelet properties and reduces the effect of the component interactions. Moreover, by

investigating the FID signal in the time-frequency domain, the main quantification problems in biomedical MRS, such as overlapping resonances are addressed.

A poor signal-to-noise ratio may hinder this operation, but since, as shown here, the MRS parameter values of a previously known number of components of the FID signal can be computed, the proposed classical solution is sufficient to reduce noise in the data. The use of the quantification procedures remain valid and the changes on the apparent relaxation time values due to the application of the low-pass filter are recovered.

The practical examples presented show that the method is suitable for different kinds of FID signals and their specific problems. Results obtained to date demonstrate the estimation accuracy of the WT method. Computation time depends on the complexity of the signal, on the number of its components and obviously on the computer power. Computation time may be reduced if the components do not overlap.

## ACKNOWLEDGMENTS

This work has been supported by a grant from Bruker Spectrospin S.A (Wissenbourg, France), by a "Programme Hospitalier de Recherche Clinique" from the French Ministry of Health and by a E.U Biomed programme.

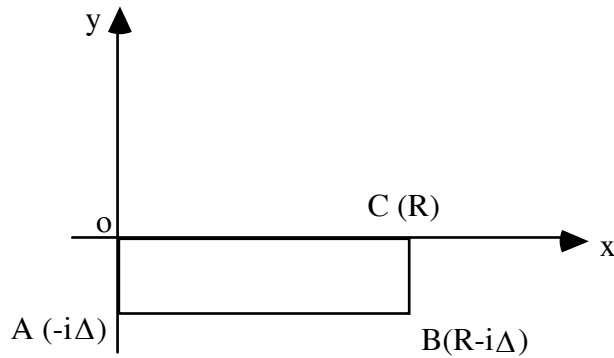
## APPENDIX 1

This appendix provides the computation of the integral  $I = \int_{\alpha}^{\infty} e^{\left(\frac{-t^2}{2} + i\Delta t\right)} dt$ .  $\alpha = \left(\frac{a}{T_2^*} - \frac{b}{a}\right)$ . I

may be written as :

$$I = \int_0^{\infty} e^{\left(\frac{-t^2}{2} + i\Delta t\right)} dt - \int_0^{\alpha} e^{\left(\frac{-t^2}{2} + i\Delta t\right)} dt = I_1 - I_2 \quad \forall \alpha \quad [40]$$

Considering the following rectangle (OABC) :



Let  $f(z)$  be a complex function under the above rectangle, given by,  $f(z) = e^{\frac{-z^2}{2}}$ , where

$z = t - i\Delta$  and  $t$  runs from  $0$  to  $\infty$ .  $I_1$  may be written as :

$$I_1 = e^{\frac{-\Delta^2}{2}} \int_{-i\Delta}^{\infty - i\Delta} e^{\frac{-z^2}{2}} dz. \quad [41]$$

The function  $z \rightarrow e^{\left(\frac{-z^2}{2}\right)}$  is analytical on and inside the rectangle OABCO. Using the Cauchy theorem, we have :

$$\oint_{OABCO} f(z)dz = \int_{OA} e^{\frac{-z^2}{2}} dz + \int_{AB} e^{\frac{-z^2}{2}} dz + \int_{BC} e^{\frac{-z^2}{2}} dz + \int_{CO} e^{\frac{-z^2}{2}} dz = 0 \quad [42]$$

1) On the segment OA of the rectangle,  $z = -iy$ , where  $y$  runs from 0 to  $\Delta$ . With respect to the sign of  $\Delta$  and using the polar co-ordinates ( $r \in [0, \sqrt{2}\Delta]$ ,  $\theta \in [0, \frac{\pi}{2}]$ ), the function  $f(z)$  on OA is given by :

$$\int_{OA} e^{\frac{-z^2}{2}} dz = \int_0^{\Delta} -ie^{\frac{y^2}{2}} dy \approx m \left[ \frac{\pi}{2} [e^{\Delta^2} - 1] \right]^{\frac{1}{2}} \quad [43]$$

2) On the segment AB we have  $z = x - i\Delta$ ,  $x \in [0, R]$ . We may write :

$$\int_{AB} e^{\frac{-z^2}{2}} dz = \int_{-i\Delta}^{R-i\Delta} e^{\frac{-1}{2}(x-i\Delta)^2} dx \quad [44]$$

Eq. [44] is equal to  $I_1$  up to the term  $e^{\frac{-\Delta^2}{2}}$ .

3) On BC segment,  $z = R - iy$  and  $y \in [\Delta, 0]$ . Thus :

$$\int_{BC} e^{\frac{-z^2}{2}} dz = -i \int_{\Delta}^0 e^{\frac{-1}{2}(R-iy)^2} dy = -ie^{\frac{-R^2}{2}} \int_{\Delta}^0 e^{\frac{y^2}{2} + iRy} dy \quad [45]$$

Eq. [45] may be overestimated by :

$$\int_{BC} f(z)dz \leq -ie^{\frac{-R^2}{2}} \int_{\Delta}^0 e^{\frac{y^2}{2}} dy. \quad [46]$$

The integral  $\int_{\Delta}^0 e^{-\frac{y^2}{2}} dy$  has a finite value, hence Eq. [46] decrease to zero when  $R \rightarrow \infty$ .

4) On segment CO,  $z = x$ , with  $x \in [R, 0]$ . Using the polar co-ordinates ( $r \in [0, \sqrt{2}\Delta]$ ,  $\theta \in [0, \pi/2]$ ), we obtain :

$$\int_{CO} e^{-\frac{z^2}{2}} dz = -\int_0^R e^{-\frac{x^2}{2}} dx \approx -\left[\sqrt{\frac{\pi}{2}} [1 - e^{-R^2}]\right]^{\frac{1}{2}} \quad [47]$$

Eq. [47] approaches  $-\sqrt{\frac{\pi}{2}}$  when  $R \rightarrow \infty$ .

Substituting the values of Eqs. [43], [44], [46] and [47] in Eq. [42], we obtain :

$$I_1 \approx \begin{cases} \sqrt{\frac{\pi}{2}} e^{-\Delta^2/2} [1 + i\sqrt{e^{\Delta^2} - 1}] & \text{if } \Delta > 0 \\ \sqrt{\frac{\pi}{2}} e^{-\Delta^2/2} [1 - i\sqrt{e^{\Delta^2} - 1}] & \text{if } \Delta < 0 \end{cases} \quad [48]$$

For  $I_2$  equal to  $\int_0^{\alpha} e^{-\frac{t^2}{2}} e^{i\Delta t} dt$ , we use the Taylor series expansion of the term  $e^{i\Delta t}$ .

$$I_2 = \int_0^{\alpha} \left[ \sum_{k=0}^{\infty} \frac{(i\Delta t)^k}{k!} \right] e^{-\frac{t^2}{2}} dt = \sum_{k=0}^{\infty} \frac{(i\Delta)^k}{k!} \int_0^{\alpha} t^k e^{-\frac{t^2}{2}} dt = \sum_{k=0}^{\infty} \frac{(i\Delta)^k}{k!} U_k \quad [49]$$

where  $U_k = \int_0^{\alpha} t^k e^{-\frac{t^2}{2}} dt$ . If  $k = 0$ , using the polar co-ordinates, it is shown that :

$$U_0 = \int_0^{\alpha} e^{\frac{-t^2}{2}} dt \approx \left\{ \begin{array}{l} \sqrt{\frac{\pi}{2}} \sqrt{1 - e^{-\alpha^2}} \text{ if } \alpha > 0 \\ -\sqrt{\frac{\pi}{2}} \sqrt{1 - e^{-\alpha^2}} \text{ if } \alpha < 0 \end{array} \right\}$$

$$U_1 = \int_0^{\alpha} t e^{\frac{-t^2}{2}} dt = \left[ 1 - e^{\frac{-\alpha^2}{2}} \right]$$

If  $k = 1$ , by using changing variables, we obtain :

The general term for this series for  $k \geq 2$ , is given by :

$$\begin{aligned} U_k &= \int_0^{\alpha} t^k e^{\frac{-t^2}{2}} dt = -\int_0^{\alpha} t^{k-1} (e^{\frac{-t^2}{2}})' dt = -\alpha^{k-1} e^{\frac{-\alpha^2}{2}} + (k-1) \int_0^{\alpha} t^{k-2} e^{\frac{-t^2}{2}} dt \\ &= -\alpha^{k-1} e^{\frac{-\alpha^2}{2}} + (k-1)U_{k-2} \end{aligned} \quad [50]$$

The series  $\sum_{k=0}^{\infty} \frac{(i\Delta)^k}{k!} U_k$  is recurrent and convergent. Combining Eqs. [40], [48], and [49],

$I$  is approximated to :

$$I \approx \left[ \sqrt{\frac{\pi}{2}} e^{\frac{-\Delta^2}{2}} (1 \pm i\sqrt{e^{\Delta^2} - 1}) \right] - \sum_{k=0}^{\infty} \frac{(i\Delta)^k}{k!} U_k \quad \forall \alpha \quad [51]$$

Eq. [51] may be described by :  $I = [B + iC]$ , where  $B$  is :

$$B = \sqrt{\frac{\pi}{2}} e^{\frac{-\Delta^2}{2}} m \sqrt{\frac{\pi}{2}} \sqrt{1 - e^{-\alpha^2}} - \sum_{k=2}^{\infty} \frac{(i\Delta)^k}{k!} U_k \quad (\text{k pair}) \quad [52]$$

and

$$C = \pm \sqrt{\frac{\pi}{2}} e^{-\frac{\Delta^2}{2}} (\sqrt{e^{\Delta^2} - 1}) - \Delta (1 - e^{-\frac{\alpha^2}{2}}) - \sum_{k=2}^{\infty} \frac{(i\Delta)^k}{k!} U_k \quad (\text{k odd}) \quad [53]$$

The signs  $m$  and  $\pm$  are conditioned by the signs of  $\alpha$  and  $\Delta$  respectively.

Note that the term  $C$  is null, if  $\Delta = 0$ . If we restrict  $k = 1$ ,  $B$  and  $C$  become :

$$B = \sqrt{\frac{\pi}{2}} e^{-\frac{\Delta^2}{2}} m \sqrt{\frac{\pi}{2}} \sqrt{1 - e^{-\alpha^2}} \quad \text{and} \quad C = \pm \sqrt{\frac{\pi}{2}} e^{-\frac{\Delta^2}{2}} (\sqrt{e^{\Delta^2} - 1}) - \Delta (1 - e^{-\frac{\alpha^2}{2}})$$

APPENDIX 2

In this appendix we investigate the term  $\frac{d(\text{Arctg}(\frac{C}{B}))}{db}$ . If we restrict the series  $U_k$  to its first two terms ( $k = 1$ ), we obtain :

$$\text{Arctg}\left(\frac{C}{B}\right) = \text{Arctg}\left[\frac{\pm\sqrt{\frac{\pi}{2}}e^{-\frac{\Delta^2}{2}}(\sqrt{e^{\Delta^2}-1})-\Delta(1-e^{-\frac{\alpha^2}{2}})}{\sqrt{\frac{\pi}{2}}e^{-\frac{\Delta^2}{2}}m\sqrt{\frac{\pi}{2}}\sqrt{1-e^{-\alpha^2}}}\right] \quad [54]$$

Writing  $\frac{d(\text{Arctg}(\frac{C}{B}))}{db}$  as a function of  $\alpha$ , ( $\alpha = \frac{a}{T2^*} - \frac{b}{a}$ ), we obtain :

$$\frac{d(\text{Arctg}(\frac{C}{B}))}{db} = \frac{e^{-\frac{\alpha^2}{2}}\left[\frac{\Delta}{a}\alpha B - C\left[\pm\frac{1}{a}\sqrt{\frac{\pi}{2}}\alpha e^{-\frac{\alpha^2}{2}}\sqrt{1-e^{-\alpha^2}}\right]\right]}{B^2 + C^2} \quad [55]$$

The denominator of Eq. [55] is different from zero.

The term  $\frac{\Delta}{a}\alpha B - C\left[\pm\frac{1}{a}\sqrt{\frac{\pi}{2}}\alpha e^{-\frac{\alpha^2}{2}}\sqrt{1-e^{-\alpha^2}}\right]$  has a finite value, it becomes equal to zero if  $\Delta = 0$ . The numerator of Eq. [55] approaches zero if the value of  $|\alpha|$  becomes larger. For a large value of  $b$  noted  $b_r$ , the factor  $e^{-\frac{\alpha^2}{2}}$  is negligible for  $b > b_r$  which implies that the function in Eq. [55] decreases to zero.

## REFERENCES

1. A. GROSSMANN AND J. MORLET, *Siam. J. Math. Anal.*, **15**, 723 (1984).
2. H. BARKHUIJSEN, R. DE BEER AND D. VAN ORMONDT, *J. Magn. Reson.*, **73**, 553 (1987).
3. J. C. HOCH, *Methods in Enzymology*, **176**, 216 (1989).
4. R. DE BEER AND D. VAN ORMONDT, in "NMR Basic Principles and Progress," **26**, pp 201-247, Springer-Verlag, Berlin Heidelberg, 1992.
5. A. DIOP, Y. ZAIMWADGHIRI, A. BRIGUET AND D. GRAVERON-DEMILLY, *J. Magn. Reson.*, **105 (B)**, 17 (1994).
6. A. GROSSMANN, R. KRONLAND-MARTINET, AND J. MORLET, in "Wavelets," (J. M. Combes, A. Grossmann, and Ph. Tchamitchian, Eds.), pp.1-20, Springer-Verlag, Marseille, 1987.
7. P. GUILLEMAIN, R. KRONLAND-MARTINET, AND B. MARTENS, in "Wavelets and Applications," (Y. Meyer, Ed.), pp 39-60, Masson, Marseille, 1989.
8. D. S. STEPHENSON, *Progress in NMR Spectroscopy*, **20**, 515 (1988).
9. N. DELPRAT, B. ESCUDIE, Ph. GUILLEMAIN, R. KRONLAND-MARTINET, Ph. TCHAMITCHIAN AND B. TORRESANI, *IEEE. Trans. Inform. Thoery.*, **38**, 644 (1992).
10. S. MALLAT, AND W. L. HWANG, *IEEE. Trans. Info. Theory.*, **38**, 617 (1992).
11. I. DAUBECHIES, *IEEE. Trans. Inform. Theory.*, **36**, 961 (1990).
12. S. L. MARPLE, *Proc. IEEE .*, **70**, 1238 (1982).
13. B. TORRESANI, in "Wavelets and Applications," (Y.Meyer, Ed.), pp 12-27, Springer-Verlag, Marseille, 1989.
14. D. W. MARQUARDT, *J. Soc. Indust. Appl. Math.*, **11**, 431 (1963).

15. A. VANDENBOS, in "Handbook of Measurement Science," (P.H.Sydenham, Ed.),  
1, pp 331-377, J. Wiley & Sons Ltd, London, 1982.
16. A.PAPOULIS, "Probability, Random Variables, and Stochastic Processes,"  
Chap.10, McGraw-Hill, N-Y, 1984.
17. J. C. HASELGROVE, V. HARIHARA SUBRAMANIAN, R. CHRISTEN AND J.  
S. LEIGH, *Rev. Magn. Res. Med.*, **2**, 167 (1987).
18. A. E. DEROME, "Modern NMR Techniques for Chemistry Research" Organic  
Chemistry series, Chap. 6, Pergamon Press, 1987.
19. J. H. J. LECLERC, *J. Magn. Reson.*, **100**, 171 (1992).
20. S. L. MARPLE, "Digital Spectral Analysis", Chap. 8, Prentice-Hall, Englewood  
Cliffs, N-J, 1987.
21. J. W. C. VAN DER VEEN, R. DE BEER, P. R. LUYTEN AND D. VAN  
ORMONDT, *Magn. Reson. Med.*, **6**, 92 (1988).
22. A. KINJN, R. DE BEER AND D. VAN ORMONDT, *J. Magn. Reson.*, **97**, 444  
(1992).

